

Texture Feature Extraction using Slant-Hadamard Transform

M. J. Nassiri, A. Vafaei, and A. Monadjemi

Abstract—Random and natural textures classification is still one of the biggest challenges in the field of image processing and pattern recognition. In this paper, texture feature extraction using Slant Hadamard Transform was studied and compared to other signal processing-based texture classification schemes. A parametric SHT was also introduced and employed for natural textures feature extraction. We showed that a subtly modified parametric SHT can outperform ordinary Walsh-Hadamard transform and discrete cosine transform. Experiments were carried out on a subset of Vistex random natural texture images using a KNN classifier.

Keywords—Texture Analysis, Slant Transform, Hadamard, DCT.

I. INTRODUCTION

TEXTURE can be used in the analysis of images in several ways: in the segmentation of scenes into distinct objects and regions, in the classification or recognition of surface materials in detection of defects and abnormalities, and in the computation of shape from surface. Although an implicitly known term, an exact definition of texture either as a surface property or as an image property has never been adequately given. Although the concept of a surface texture as a pattern of variations in macroscopic surface topology is easy to accept, real-world surface textures are extremely difficult to model mathematically. Texture modeling as a function of surface attributes is yet more complex, since an accurate model must incorporate descriptions of both the optical properties of the surface materials and of the geometries of the lighting sources and imaging system. In general, real texture modeling is a complex and hard to solve problem, regarding infinite combination of illumination, reflexes, surface topologies, shadows, and so on.

Texture analysis has been studied for many years and vast studies have been accomplished in this field. In a more comprehensive categorizations, Tuceryan and Jain [14] distinguish four different approaches to texture analysis: statistical, geometrical, model-based and signal processing approaches [4]. All of the described methods in this study case signal processing-based. They consider the texture to be analyzed as a 2D or 3D matrix and apply signal processing algorithms on it.

In this paper a new texture feature extraction scheme called Slant-Hadamard Transform (SHT) will be introduced. We describe and compare SHT with two other feature extractors, ordinary Walsh-Hadamard Transform (WHT) and Discrete Cosine Transform (DCT), to show its advantages in texture classification.

Authors are with Department of Computer Engineering, University of Isfahan, Isfahan, 81746, Iran (e-mails: {nassiri, abbas_vafaei, monadjemi}@eng.ui.ac.ir).

Historically, Enomoto and Shibata [3] conceived the first, eight points slant transform in 1971. Its major innovation is given by the slant vector, which can properly follow gradual changes in brightness of natural images. Since its development, Pratt, Welch, and Chen [5,6] have generalized it. They presented a procedure for computing the slant transform matrix of order 2^n . The slant transform has the best compaction performance amongst the non-sinusoidal fast orthogonal transforms, but it is not the best in its performance measure [1]. In general, there is a tradeoff between time and its computational complexity. Therefore, the Slant-Hadamard Transforms improvement schemes that yield performance comparable to that of the DCT without incurring their computational complexity have been developed. This transform is parametric and proposed by Aguin et.al [1]. This parametric class performs better in generalized Wiener filtering than existing Slant-Hadamard transforms for the first-order Markov and generalized image correlation models [1].

This paper has been organized as below: Slant-Hadamard transform is introduced in Section 2. Texture features is described in Section 3. In Section 4, we illustrate the performance of rival schemes in texture classification. The paper will be concluded in section 5.

II. SLANT HADAMARD TRANSFORM

This section briefly reviews the Slant Hadamard Transform (SHT) and its background. Many digital signal and image processing concepts, such as transmission and processing, filtering, compression, encoding, restoration, and enhancement of images and signals, require the use of fast unitary transforms such as the Walsh Hadamard Transform (WHT). However, a phenomenon characteristic of digital images is the presence of approximately constant or uniformly changing grey levels over a considerable distance or area which is not completely match the WHT property of sharp changes [2]. The slant transform is specifically defined for efficient representation of such signals. It is a piecewise linear basis that follows the spirit of the Walsh transform, possessing a discrete saw tooth-like basis vector, which efficiently represents linear brightness variations along an image line. This transform has been used for signal compression [5,6], pattern recognition [9,12], and in Intel's 'Indo' video compression algorithm [13]. With this background, Slant Transform is defined to have the following properties:

1. An orthonormal set of basis vectors (A subset $\{v_1, \dots, v_k\}$ of a vector space V which is called orthonormal if the inner product $\langle v_i, v_j \rangle = 0$ when $i \neq j$).
2. One constant basis vector (The first row of slant matrix is constant basis vector).

3. One slant basis vector. (The second row of slant basis matrix is slant basis vector).
4. The sequency property (the sequency of base vector is equal to the sign change number of its elements).
5. Variable size transformation.
6. A fast computational algorithm.
7. High energy compaction (A major attribute of an image transform is that the transform compact the image energy to a few of the transform domain samples. A high degree of energy compaction will result if the basis vectors of the transform matrix "resemble" typical horizontal or vertical lines of an image) [16].

The Slant Transform definition and its properties are given in [5], [6].

This has stimulated the construction of a new class of custom-built fast unitary transforms as follows: The forward and inverse slant Hadamard transforms of order $N = 2^n$ for $(n=1,2,3,\dots)$, are defined as $X = S_{2^n} x, x = S_{2^n}^T X$, where S_{2^n} is generated recursively [5,6]:

$$S_{2^n} = \frac{1}{\sqrt{2}} Q_{2^n} \begin{bmatrix} S_{2^{n-1}} & O_{2^{n-1}} \\ O_{2^{n-1}} & S_{2^{n-1}} \end{bmatrix} = \frac{1}{\sqrt{2}} Q_{2^n} (I \otimes S_{2^{n-1}}), \quad (1)$$

where O_M denotes the $M \times M$ zero matrix, \otimes denotes the Kronecker operator product, and the Q_{2^n} is the recursion kernel matrix defined as:

$$Q_{2^n} = \begin{bmatrix} 1 & 0 & O_0 & 1 & 0 & O_0 \\ a_{2^n} & b_{2^n} & O_0 & -a_{2^n} & b_{2^n} & O_0 \\ O^0 & O^0 & I_{2^{n-1}-2} & O^0 & O^0 & I_{2^{n-1}-2} \\ 0 & 1 & O_0 & 0 & -1 & O_0 \\ -b_{2^n} & a_{2^n} & O_0 & b_{2^n} & a_{2^n} & O_0 \\ O^0 & O^0 & I_{2^{n-1}-2} & O^0 & O^0 & -I_{2^{n-1}-2} \end{bmatrix} \quad (2)$$

where $2^n > 2$, I_m denotes an identity matrix of order m , O^0, O_0 are row and column zero vectors respectively, and the parameters a_{2^n} and b_{2^n} are obtained recursively by:

$$a_{2^n} = \sqrt{\frac{3(2^{2n-2})}{4(2^{2n-2}) - \beta_{2^n}}}, \quad b_{2^n} = \sqrt{\frac{(2^{2n-2}) - \beta_{2^n}}{4(2^{2n-2}) - \beta_{2^n}}} \quad (3)$$

Where $a_2 = 1, -2^{2n-2} \leq \beta_{2^n} \leq 2^{2n-2}$ [10].

The parametric slant transforms fall into one of at least four different categories, depending on the β_{2^n} value chosen, and they are considered as special cases of Slant-Hadamard and Hadamard Transforms of order 2^n for instance:

1. For $\beta_4 = \beta_8 = \dots = \beta_{2^n} = \beta = 1$ we obtain the classical slant transform [3, 9].
2. For $\beta_{2^n} = 2^{2n-2}$ for all $\beta_{2^n}, n \geq 2$, we obtain the ordinary WHT [8].

3. For $\beta_4 = \beta_8 = \dots = \beta_{2^n} = \beta, \beta \leq |4|$, we refer to this case as the *constant-beta* slant transform [9].
4. For $\beta_4 \neq \beta_8 \neq \dots \neq \beta_{2^n}, -2^{2n-2} \leq \beta_{2^n} \leq 2^{2n-2}, n=2,3,4,\dots$, we refer to this case as *multiple-beta* slant transform. In this case, some of β_{2^n} can be equal but not all of them.

III. TEXTURE FEATURES

In this section, we briefly introduce three competitive feature extractors used in this study: Discrete Cosine Transform, ordinary Walsh/Hadamard Transform, and the proposed Slant Hadamard Transform-based method.

A. Discrete Cosine Transform

Most of current approaches to the texture feature extraction problem employ statistical methods such as co-occurrence matrices or Local Binary Patterns[17]. For the analysis of a texture image, statistical methods usually require large storage and a lot of computation to calculate the feature vectors. For solving these problems, some researchers have employed signal processing-based methods like DCT for texture representation. DCT shows that it is a practical and reliable method for image and texture feature extraction as well as compression in many applications [7].

To apply the DCT transform, we firstly convert an RGB image into gray level. The two dimensional DCT then can be written in terms of pixel values $f(i,j)$ for $i,j = 0,1,\dots, N-1$ and the frequency-domain transform coefficients (i.e. DCT coefficients) $F(u,v)$ would be:

$$F(u,v) = \frac{1}{\sqrt{2N}} C(u)C(v) \sum_{i=0}^{N-1} \sum_{j=0}^{N-1} f(i,j) \times \cos\left[\frac{(2i+1)u\pi}{2N}\right] \cos\left[\frac{(2j+1)v\pi}{2N}\right] \quad (4)$$

For $u, v = 0, 1, \dots, N-1$

Where

$$c(x) = \begin{cases} \frac{1}{\sqrt{2}} & \text{for } x = 0 \\ 1 & \text{otherwise} \end{cases}$$

As equation 4 shows, DCT also is a real transform.

As Fig. 1.b and c depict, in the DCT transform domain, lower frequency coefficients gather at the top-left corner and higher frequency ones at the bottom-right corner of the transformed matrix.

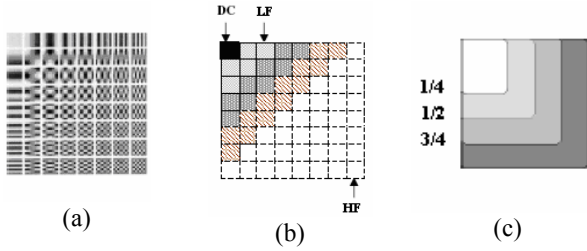


Fig. 1 (a) DCT Basis Pattern, (b) Increment of frequency, (c) Frequency bands in the DCT domain

We extract a 10 component feature vector from each transformed image. The first two features are the mean (μ) and standard deviation (δ) of $F(u,v)$. We also divided $F(u,v)$ into four frequency bands using equidistance 1/4 margins and compute the μ and δ of each band to obtain eight more features (see Fig. 1.c).

B. Ordinary WHT Features

Amongst the family of orthogonal linear transforms of time/spatial domain signals, which mostly employ sinusoidal-based kernel functions (e.g. Fourier or DCT), the Walsh Hadamard Transform (WHT) which employs rectangular kernel function is relatively different case. The natural Hadamard Matrix is defined recursively as below:

$$H_1 = \frac{1}{\sqrt{2}} \begin{bmatrix} 1 & 1 \\ 1 & -1 \end{bmatrix} \quad (5)$$

$$H_n = H_1 \otimes H_{n-1} = \begin{bmatrix} H_{n-1} & H_{n-1} \\ H_{n-1} & -H_{n-1} \end{bmatrix} \quad (6)$$

The Hadamard matrix can also be obtained by defining its element in the k_{th} row and m_{th} column of H ($k, m = 0, 1, \dots, N-1$) as

$$h(k, m) = (-1)^{\sum_{i=0}^{n-1} k_i m_i} = \prod_{i=0}^{n-1} (-1)^{k_i m_i} = h(m, k) \quad (7)$$

Where

$$k = \sum_{i=0}^{n-1} k_i 2^i = (k_{n-1} k_{n-2} \dots k_1 k_0)_2 \quad (k_i = 0, 1) \quad (8)$$

$$m = \sum_{i=0}^{n-1} m_i 2^i = (m_{n-1} m_{n-2} \dots m_1 m_0)_2 \quad (m_i = 0, 1) \quad (9)$$

We used a *sequency-ordered Hadamard* matrix, where the rows (and columns) are ordered according to their sequency, i.e. in the first row there are no sign changes, and in the n_{th} row there are $n-1$, e.g. see Fig. 3.a. The 2D Walsh-Hadamard transform can be defined as $WHT(f) = HfH'$ where f is the image and H and H' are the Hadamard matrix and its transpose. Note that for a Hadamard matrix $H = H'$. Apart from the substitution of the sequence concept instead of the frequency, the distribution of the transform domain coefficients is similar with the DCT.

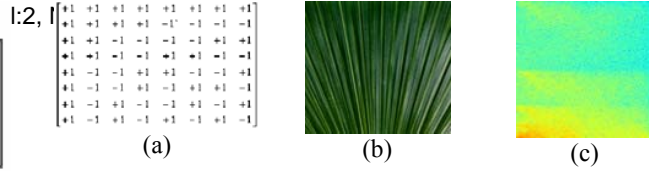


Fig. 2 (a) Sequency ordered 8×8 Hadamard matrix H_8 , (b) a texture, (c) its Hadamard transform

There are some simple algorithms to convert a natural Hadamard matrix to a sequency ordered one [4]. Fig. 2.a depicts an 8×8 sequency ordered Hadamard matrix. In our experiments we also extracted a 10 component feature vector from each input image. They were the global μ and δ , along with the μ and δ of 4 respective sequency bands.

C. SHT Features

As we described in section 2, SHT is a parametric transform where we can gain different characteristics from a unique transform by changing its parameters. For instance, Fig. 3 shows an 8×8 SHT matrix with $\beta_4 = \beta_8 = 1$, and the rows of a 16×16 SHT matrix. As mentioned before, row 0 and row 1 of the SHT matrix include the constant and slant basis vector respectively. By changing the β s we can produce different transform matrices, therefore have various properties in the transform domain. SHT feature vectors contained the global and 4-band μ and δ too (10 components).

$$\begin{bmatrix} 0.3536 & 0.3536 & 0.3536 & 0.3536 & 0.3536 & 0.3536 & 0.3536 & 0.3536 \\ 0.5401 & 0.3858 & 0.2315 & 0.0772 & -0.0772 & -0.2315 & -0.3858 & -0.5401 \\ 0.3536 & -0.3536 & -0.3536 & 0.3536 & 0.3536 & -0.3536 & -0.3536 & 0.3536 \\ 0.1581 & -0.4743 & 0.4743 & -0.1581 & 0.1581 & -0.4743 & 0.4743 & -0.1581 \\ 0.4743 & 0.1581 & -0.1581 & -0.4743 & -0.4743 & -0.1581 & 0.1581 & 0.4743 \\ 0.2415 & -0.0345 & -0.3105 & -0.5866 & 0.5866 & 0.3105 & 0.0345 & -0.2415 \\ 0.3536 & -0.3536 & -0.3536 & 0.3536 & -0.3536 & 0.3536 & 0.3536 & -0.3536 \\ 0.1581 & -0.4743 & 0.4743 & -0.1581 & -0.1581 & 0.4743 & -0.4743 & 0.1581 \end{bmatrix}$$

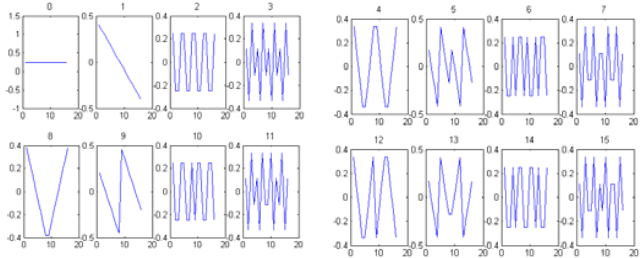


Fig. 3 An 8×8 Slant Hadamard matrix (top), and rows of a 16×16 SHT matrix (bottom)

IV. EXPERIMENTAL RESULTS

A set of textures from the Vistex test suite [15] is used in our classification experiments. Some samples of this set is shown in Fig. 4. The total number of images is 10, each with the resolution of 512×512 pixels and converted to 256 gray levels. Each image was subdivided into 16 (4 by 4) adjacent but non-overlapping patches of 128×128 pixels. Then eight patches (50%) were selected to from the training set for the classifiers.



Fig. 4 Some sample textures from our dataset

We used a k-Nearest-Neighborhood (kNN) classifier and leave-one-out method in all experiments [4]. Before feeding to the classifier, each feature was normalized to zero-DC over all samples in the set. The kNN classifier has several advantages over the alternatives such as the artificial neural networks, e.g. no training is required and the results are repeatable. There also is only one tunable parameter, k. In this study we performed the classification tests with k=3.

TABLE I
CLASSIFICATION RESULTS USING ADJACENT (ODD-EVEN)
TRAINING/TESTING SAMPLES DIVISION

Feature extraction scheme	PARAMETER SET OR SIZE	No. IC (out of 80)	CA
Parametric Slant-Hadamard	$\beta_4 = 2^2, \beta_8 = 2^4, \beta_{16} = 2^6, \beta_{32} = 2^8, \beta_{64} = 2^{10}, \beta_{128} = 2^{12}$	2	%97.5
Parametric Slant-Hadamard (Constant beta)	$\beta_4 = \beta_8 = \beta_{16} = \beta_{32} = \beta_{64} = \beta_{128} = 2$	4	%95
Parametric Slant-Hadamard (Classical)	$\beta_4 = \beta_8 = \beta_{16} = \beta_{32} = \beta_{64} = \beta_{128} = 1$	5	%93.75
Ordinary Walsh/Hadamard transform	128x128	3	%96.25
DCT	128x128	3	%96.25

Table I shows the classification results using adjacent (odd-even) training /testing patches. In this table (as well as Table II) No.IC is the number of incorrect classification (out of 80), and CA is the classification accuracy (percent).

As this table suggests, the best performance is achieved by the parametric SHT with CA=97.5% or just 2 incorrect class assignment out of 80 samples. The parameter set is also presented in this table and suggests that starting with smaller 2^n for the first β s and moving towards the larger one (e.g. 2^2 to 2^{12}) will provide the best classification accuracy. This parameter set has been found by trial and error.

Vol:2, No:5, 2008
The WHT and DCT performed better (both with CA= 96.25%), rather than the SHT with constant β s (95%), and the classical SHT (93.75%).

Then, the experiment was repeated, this time with the upper eight patches of each texture as the training, and lower eights as the testing set. We expected a slightly lower performance compared to the first test due to more diversity between the training and testing set. Table II depicts the outcomes, where again the best features extractor was the parametric SHT with 97.5% classification accuracy. The optimum parameter set however is a bit different from the first test.

Meanwhile, the classical SHT was the next accurate feature extractor with CA=96.25%, which slightly outperforms other methods.

To sum up, we can suggest that the parametric SHT, if its parameter set precisely, will be a high performance texture analyzer. On the other hand, a wrongly set parameter can decrease its accuracy even lower than the very simple WHT.

TABLE II
CLASSIFICATION RESULTS USING UPPER-LOWER HALF TRAINING/TESTING
SAMPLES DIVISION

Feature extraction scheme	PARAMETER SET OR SIZE	No. IC (out of 80)	CA
Parametric Slant-Hadamard	$\beta_4 = 2^2 - 1, \beta_8 = 2^4 - 2, \beta_{16} = 2^6 - 1.85, \beta_{32} = 2^8, \beta_{64} = 2^{10}, \beta_{128} = 2^{12}$	2	%97.5
Parametric Slant-Hadamard (Constant beta)	$\beta_4 = \beta_8 = \beta_{16} = \beta_{32} = \beta_{64} = \beta_{128} = 2$	5	%93.75
Parametric Slant-Hadamard (Classical)	$\beta_4 = \beta_8 = \beta_{16} = \beta_{32} = \beta_{64} = \beta_{128} = 1$	3	%96.25
Ordinary Walsh/Hadamard transform	128x128	4	%95
DCT	128x128	5	%93.75

V. CONCLUSION

In this paper, we introduced a new application for the SHT, which is texture feature extraction. We showed that amongst different signal processing-based real, fast texture analyzers, e.g. WHT, DCT, and SHT, a parametric SHT shows a considerably high performance. We also determined the importance of the parameter setting to obtain effective features. Tests were focused on natural random textures classification, where the classification challenge is usually more difficult. Meanwhile the classification accuracy of 97.5% using a simple kNN classifier proves the efficiency of the SHT-based proposed feature extraction scheme.

- [1] S. Agaian, K. Tourshan, and J. P. Noonan, "Parametric Slant-Hadamard Transforms With Applications", IEEE Signal Processing Letters, Vol 9, No 11, November 2002.
- [2] A. Monadjemi, B.T. Thomas, and M. Mirmehdi, "Speed v. Accuracy for High Resolution Colour Texture Classification" Proceedings of the BMVC 2002 Conference, Cardiff, Wales, Sept 2002 .
- [3] H. Enomoto and K. R. Shibata, "Orthogonal transform system for television signals", IEEE Trans, Electromagn. Compat. 13(1971), 11-17
- [4] A. Monadjemi, "Towards Efficient Texture Classification and Abnormality Detection", PHD Thesis of university of Bristol, October 2004
- [5] W.K Pratt, L.R. Welch and W.H. Chen, "Slant transform for image coding", Proc. Applications of Walsh functions, 1972
- [6] W.K Pratt, L.R. Welch and W.H. Chen, "Slant transform for image coding", IEEE Trans. Commun. 22(8) (1974), 1075-1093.
- [7] S. Lee, H. Jung Bae, and S. Hwan Jung, "Efficient Content-Based Image Retrieval Methods Using Color and Texture", ETRI Journal 20 (1998) 272-283.
- [8] N. Ahmed and K. R. Rao, "Orthogonal Transforms for Digital Signal Processing", New York: Springer-Verlag, 1975.
- [9] P. C. Mali, B. B. Chaudhuri, and D. D. Majumder, "Some properties and fast algorithms of slant transform in image processing," Signal Processing, vol. 9, pp. 233-244, 1985.
- [10] S. Agaian, K. Tourshan, and J. P. Noonan, "Partially Signal Dependent Slant Transforms for Multispectral Classification", Integrated Computer-Aided Engineering 10(2003) 23-35 IOS Press.
- [11] K. G. Beauchamp. "Applications of Walsh and Related Functions". Academic Press, 1984.
- [12] R. C. Gonzalez and R. E. Woods, "Digital Image Processing", Addison-Wesley Publishing Company, 1992.
- [13] P.C. Mali and D. D. Majumder, "An analytical comparative study of a class of discrete linear basis transforms", IEEE Trans. Syst., Man & Cyber. 24(3) (1994), 531-535.
- [14] M. Tuceryan and A. Jain. "Texture analysis". In The Handbook of Pattern Recognition and Computer Vision, pages 207-248. World Scientific, 1998.
- [15] MIT Media Lab. VisTex: Vision Texture database. Retrieved 1 Sep 2005 from the World Wide Web: <http://www.white.media.mit.edu/vismod/imager/VisionTexture/vistex.html>, 2005.
- [16] Z. Xin Hou, N. Xu, H. Chen, and X. Leili, "Fast Slant Transform With Sequency Increment and its Application in Image Compression", Proceedings of the Third International Conference on Machine Learning and Cybernetics, Shanghai, August 2004
- [17] H. Hasanpor, K. Jamshidi, and A. Monadjemi, "Steel Surface inspection using Local Binary Pattern and Color Features", 16th International Conference on Computer Theory and Applications, September 2006.